

# Dalton Transactions

Accepted Manuscript



This is an *Accepted Manuscript*, which has been through the Royal Society of Chemistry peer review process and has been accepted for publication.

*Accepted Manuscripts* are published online shortly after acceptance, before technical editing, formatting and proof reading. Using this free service, authors can make their results available to the community, in citable form, before we publish the edited article. We will replace this *Accepted Manuscript* with the edited and formatted *Advance Article* as soon as it is available.

You can find more information about *Accepted Manuscripts* in the [Information for Authors](#).

Please note that technical editing may introduce minor changes to the text and/or graphics, which may alter content. The journal's standard [Terms & Conditions](#) and the [Ethical guidelines](#) still apply. In no event shall the Royal Society of Chemistry be held responsible for any errors or omissions in this *Accepted Manuscript* or any consequences arising from the use of any information it contains.

## ARTICLE

Cite this: DOI: 10.1039/x0xx00000x

Received 00th January 2012,  
Accepted 00th January 2012

DOI: 10.1039/x0xx00000x

www.rsc.org/

## An *N*-Heterocyclic carbene phenanthroline ligand: synthesis, multi-metal coordination and spectroscopic studies.

Alyssa A. Webster,<sup>a</sup> Shyamal Prasad,<sup>b</sup> Justin M. Hodgiss<sup>\*b</sup> and John O. Hoberg<sup>\*a</sup>

Dimetal complexes of a new *N*-Heterocyclic carbene/phenanthroline ligand have been synthesized. Coordination of both ruthenium and rhenium to the phenanthroline moiety in combination with platinum at the carbene moiety are reported. Steady-state and time-resolved optical absorption and photoluminescence spectra were obtained for the complexes. These results illustrate significant changes occur with the incorporation of the second metal, and that the specific metal bound to the phenanthroline moiety is important to the photophysical characteristics of this system.

### Introduction

Dinuclear metal complexes are an interesting and important set of compounds due to their wide variety of applications. These applications include cooperative dual catalysis,<sup>1-5</sup> material science involving metal-metal communications,<sup>6-7</sup> non-linear optics<sup>8-10</sup> and water-splitting.<sup>11,12</sup> Distinct from these complexes are transition metal *N*-Heterocyclic Carbenes (NHCs). These complexes have undergone a true explosion in homogeneous catalysis,<sup>13,14</sup> and constitute “a new structural principle for catalyst design in homogeneous catalysis”.<sup>15</sup> The merging of these two areas has the potential to significantly impact the above fields of research. However, given this intriguing concept, a scarcity of reports have only just appeared, which include the incorporation of metal salen/NHC<sup>16</sup> and crown ether/NHC motifs.<sup>17</sup> Recently, we embarked on the design of a ligand capable of tandem metal coordination via a phenanthroline/NHC construct and report herein the synthesis of the ligand, its metal complexes and an application in photoinduced H<sub>2</sub> formation. As these studies were underway, Chung and co-workers reported on their work in this area.<sup>18,19</sup> In addition to an alternative synthesis, we also sought to obtain spectroscopic information on changes the second metal brought to the complex, and whether charge-transfer from one metal to the other was feasible.

The overall design of the complex is depicted in Figure 1 and provides a substantial degree of flexibility by modification of (i) the phenanthroline starting material, (ii) metal center M<sup>1</sup>, (iii) metal center M<sup>2</sup>, (iv) and structural and electronic variation of either R<sup>1</sup> or R<sup>2</sup>. An example of (i) is the modification of 1,10-phenanthroline via a one-step bromination at the 3,8 position, which undergoes facile

transmetallation reactions.<sup>20</sup> For this work, only 1,10-phenanthroline was used and variations of the metals centers M<sup>1</sup> and M<sup>2</sup> were undertaken. We also focused on the use of only alkyl groups for R<sup>1</sup> and R<sup>2</sup>.

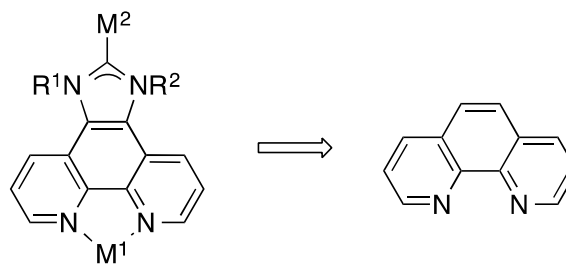


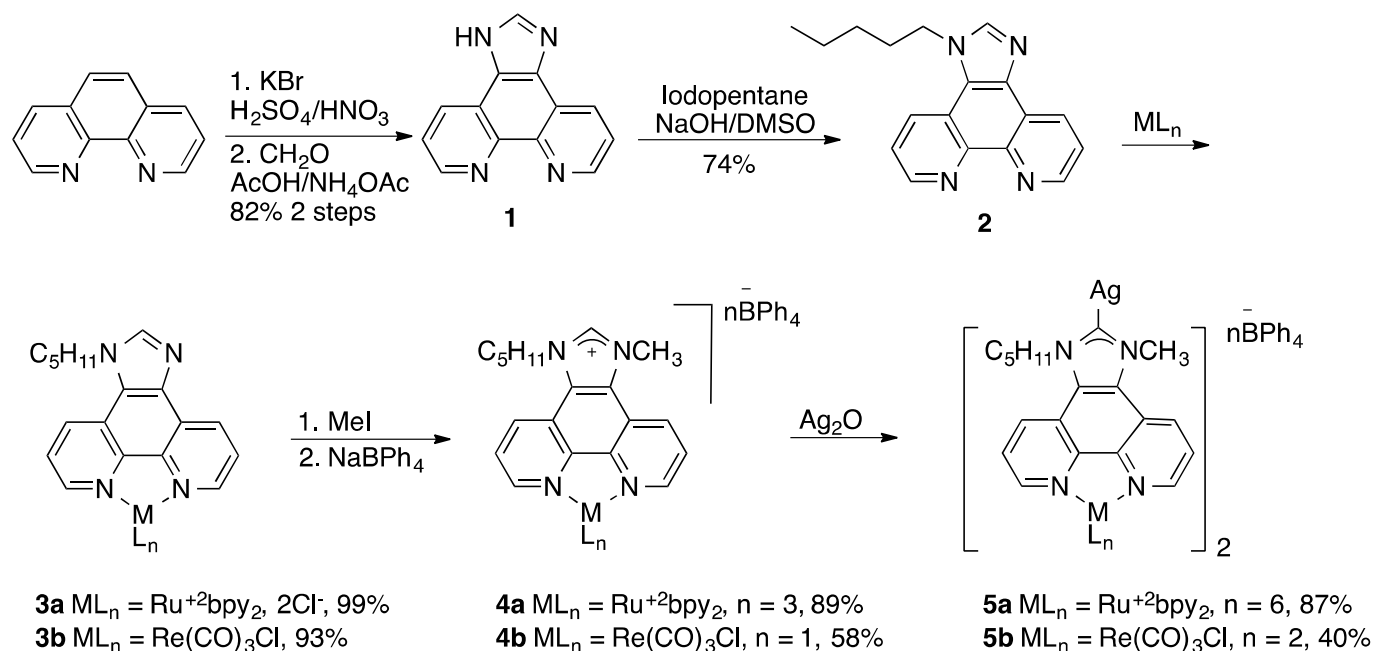
**Figure 1.** Dinuclear phenanthroline/NHC complex based on the phenanthroline scaffold.

### Results and discussion

#### Synthesis

Our synthesis began with alkylation of imidazo[4,5-*f*] 1,10-phenanthroline (**1**), which is readily prepared in two high yielding steps, Scheme 1.<sup>21,22</sup> A pentyl group was chosen for these initial studies to increase solubility, although additional groups are readily prepared. The formation of imidazolium salts of **2** were attempted, however a myriad of products were obtained upon treatment with alkyl halides. Presumably, alkylation of the phenanthroline nitrogens was taking place and thus **2** was reacted with both RuCl<sub>2</sub>(bpy)<sub>2</sub> (bpy = 2,2'-

## ARTICLE



SCHEME 1. Synthesis of metal-phenanthroline NHC silver salts.

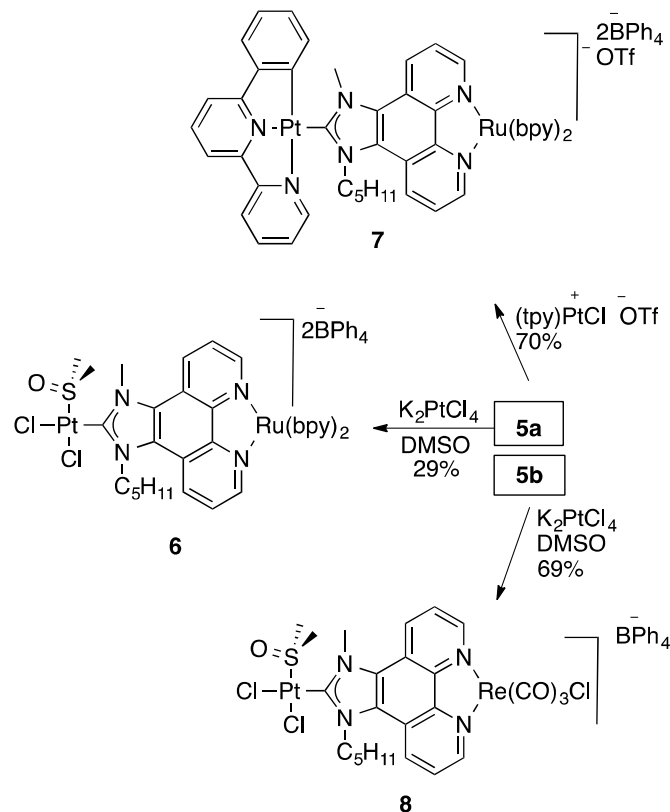
bipyridine)<sup>23</sup> and  $Re(CO)_5Cl$  to provide **3a** and **3b** respectively. Treatment with methyl iodide at 100 °C in a sealed tube gave the imidazolium salts of **3a** and **3b** as single products. Exchange of the counter ions was accomplished in facile manner to provide **4a** and **4b** in overall excellent yields. Using the procedure of Lin,<sup>24</sup> the silver salts **5a** and **5b** were formed as colored solids in both high and moderate yields. These solids are light sensitive, but if kept in the dark appear to be stable at room temperature in air. Even so, these complexes were typically exchanged with other metals immediately after formation to produce the final targets. In our studies, crystals suitable for X-ray diffraction were unattainable for any complex. Therefore, selection of a metal for exchange with the silver that would also provide concrete evidence for the formation of a metal-NHC complex was needed. As platinum is NMR active and would show coupling to the NHC carbon, formation of a platinum-NHC complex was undertaken.

The procedure adopted was initially published by Rouke and co-workers in 2007.<sup>25</sup> Thus, treatment of **5a** with  $K_2PtCl_4$  in DMSO gave clean conversion to **6** although in low yield, Scheme 2. Evidence for the formation of **6** was obtained by both  $^1H$  and  $^{13}C$  NMR. As noted by Rouke, these types of complexes maintain significant barriers of rotation about the NHC-platinum bond, giving rise to distinct  $^1H$  NMR spectra. As expected, inequivalent N-methylene protons of the pentyl group were observed. For comparison, the N-CH<sub>2</sub>- signals in complex **4a** resonate as an expected triplet at 5.0. However, with complex **6** the methylene protons appear as separate doublet of triplets at 5.5 and 5.35 with a coupling of  $J_{H,H} = 15Hz$ . Furthermore, the methyl groups of the DMSO also displayed a  $^3J_{H,Pt} = 22Hz$  value, which is in agreement with that

reported by Rouke for an NHC-DMSO cis relationship.<sup>25</sup> Further confirmation could be attained from both an HMBC and  $^{13}C$  NMR. A correlation between both the N-methyl and N-methylene protons to the carbene carbon was obtained from the HMBC. This carbon displayed a platinum-carbene coupling of  $^1J_{C,Pt} = 822Hz$ . Finally, a NOESY spectrum displayed correlations between the hydrogens of the methyl group of the NHC ligand and the coordinated DMSO methyl groups.

An additional platinum-ruthenium complex was synthesized in significantly higher yield. Thus, reaction of **5a** with 2,2',2''-terpyridine platinum(I) chloride gave **7** as an orange solid in 70% yield. Proton NMR illustrated a complex aromatic region due to the added terpyridine signals. Additionally, the N-methylene protons of the pentyl group appeared as a single broad resonance at 5.0 ppm. Given the complexity of the  $^{13}C$  NMR, the Pt-carbene coupling constant could not be ascertained. However, a NOESY spectrum displayed correlations between both the N-methyl and N-pentyl groups to the terpyridine protons.

Finally, rhenium complex **5b** was also converted to the platinum-NHC dimetal species. Again treatment with  $K_2PtCl_4$  in DMSO gave **8** as a yellow solid in good yield. As in complex **6**, the N-methylene protons of **8** appeared as separate signals at 5.2 and 5.5 ppm in the  $^1H$  NMR. As before, HMBC was used to verify the structure. The relative simplicity of complex **8** allowed not only the connectivity of the N-methyl and N-methylene protons to the carbene resonance at 157ppm to be established; but their connectivity to the quaternary imidazole peaks at 127 and 126, respectively were also observed. Similar to **6**, a platinum-carbene coupling of  $^1J_{C,Pt} = 863 Hz$  was observed.



SCHEME 2. Dimetal NHC/phenanthroline complexes.

### Spectroscopic Studies

Several studies were performed to gain a better understanding of how the physical properties and both the ground and excited states changed when both **4a** and **4b** were coordinated to a second metal via the carbene moiety. The absorption spectra of the ruthenium-based **4a**, **6** and **7** are illustrated in Figure 1 and summarized in Table 1. There are two major components to each of the absorption spectra. Firstly, in the single ruthenium metal complex **4a**, light green, the high energy absorptions from 215–285 nm belong to the  $\pi$ - $\pi^*$  transitions experienced by the bipyridine and the phenanthroline imidazole (PhIm<sup>MP</sup> where M = Methyl and P = Pentyl) ligands. The second feature, the low-energy absorption band ranging from ~350–500 nm, is due to the MLCT from the d- $\pi^*$  transition of the Ru(bpy)<sub>2</sub>PhIm<sup>MP</sup> complex.

Once the second metal is coordinated to the carbene position interesting changes in the absorption spectra are observed. Primarily there was a change in the  $\pi$ - $\pi^*$  transition absorption band with the first feature from 200–245 nm in both Pt/Ru metal complexes.<sup>26</sup> The observed decrease in absorption is due to the inhibition of the  $\pi$ - $\pi^*$  transition of the PhIm<sup>MP</sup>, due to secondary metal complexation and can be rationalized by a perturbation that occurs at the PhIm<sup>MP</sup> ligand upon secondary metal coordination.<sup>26</sup> There is also an increased absorption from the  $\pi$ - $\pi^*$  absorption band from 250–285 nm. The rise in absorption is due to the increase in  $\pi$ - $\pi^*$  transitions and in complex **6** this absorption is significantly enhanced by the presence of the DMSO ligand vs the terpyridine ligand. Finally, the d- $\pi^*$  transition is significantly effected with the formation of **6** vs **7** as a noticeable absorption band at 455 nm is observed for **6**.

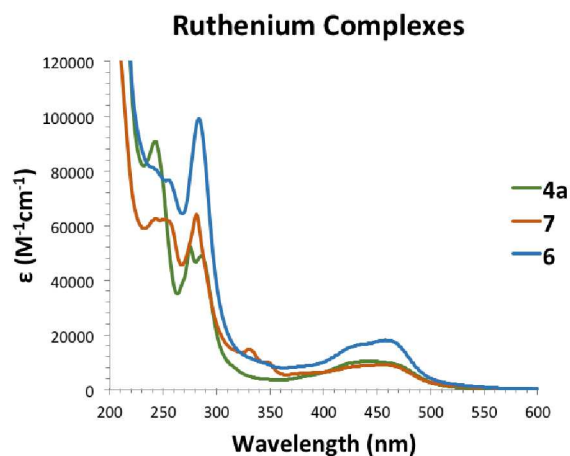


**Figure 1:** UV-Vis absorption spectra of Ruthenium-based complexes **4a**, **6** and **7**. Complexes were dissolved in MeCN.

For complex **4b** and **8** (Figure 2), a similar change was observed with an increased absorption at 400 nm. Additionally, the shoulder that appears in the mono-metallic species **4b** disappears and the absorption band becomes sharper. This can be attributed to a perturbation of the MLCT from the d(Re)  $\rightarrow$   $\pi^*$ (PhImMP) decreasing absorption at 450 nm.

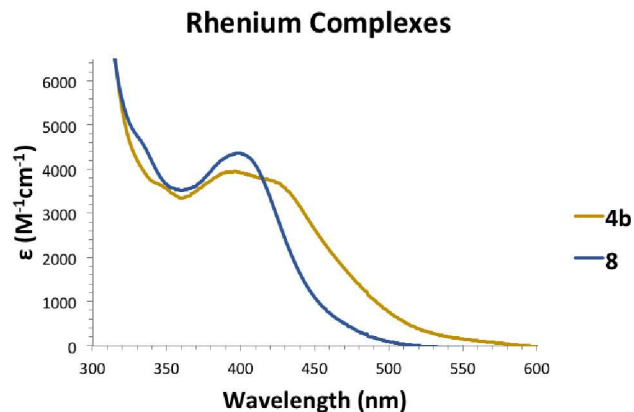


**Figure 2:** UV-Vis absorption spectra of Rhenium-based complexes **4b** and **8**.

**Table 1.** Absorption, emission properties for complexes **4**, **6**–**8**.

Complex	$\lambda_{\text{abs}}/\text{nm}$	$\epsilon/\text{M}^{-1}\text{cm}^{-1} (\times 10^4)$	$\lambda_{\text{em}}/\text{nm}$	$\phi_{\text{em}}$
<b>4a</b>	241, 274	8.9, 5.24	619	0.604
	287, 438	4.92, 1.02		
<b>6</b>	236, 282	8.17, 9.83	605	0.572
	427, 457	1.56, 1.86		
<b>7</b>	239, 280	6.14, 6.34	604	0.613
	331, 348	1.41, 0.969		
	455	0.872		
<b>4b</b>	395	0.39	582	0.156
<b>8</b>	399	0.435	570	0.138

### Emission Spectra

The emission spectra for the complexes are shown in Figures 3 and 4, and as seen the complexes show a large Stokes shift. The emission maxima and the quantum yields are estimated and summarized in Table 1. The emission quantum yields for these systems were estimated by standard calibration using Ru(bpy)<sub>3</sub>2Cl<sup>-</sup> as a standard.<sup>27</sup> A large fluorescence signal is evident for both the mono-metallic Ru(bpy)<sub>2</sub>PhIm<sup>MP</sup> complex **4a** and the di-metallic complex **6**. This increase once the second metal is attached is due to either fluorescence being the more favorable pathway for excited state decay or a decrease in non-radiative processes. However, the emission from the Re(CO)<sub>3</sub>ClPhIm<sup>MP</sup>, **4b** in yellow Figure 4, is slightly quenched upon platination, shown in dark blue.

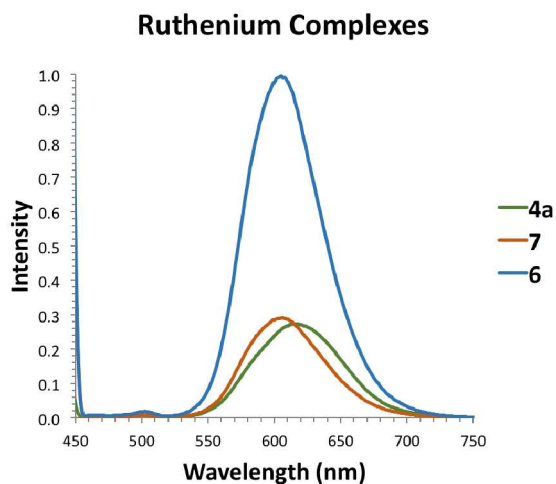


**Figure 3:** Photoluminescence of **4a**, **6** and **7** (excitation  $\lambda = 436$  nm).

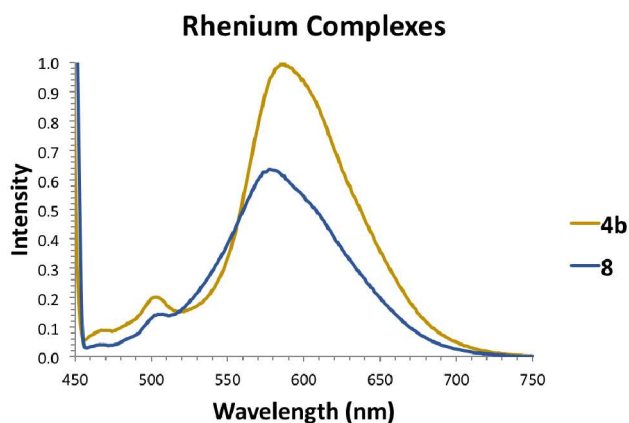


**Figure 4:** Photoluminescence of **4b** and **8** (excitation  $\lambda = 436$  nm). The minor shoulder at 500 nm is attributed to an unknown impurity.

### Transient Absorption spectroscopy

Transient absorption (TA) spectroscopy was performed in order to interrogate the nature of excited states and how they are affected by the presence of the second metal. Samples were dissolved in MeCN in a 1 mm cuvette and degassed (unless otherwise stated). Samples were excited with 355 nm (1 ns) pulsed excitation and probed with ultrafast continuum pulses in the 350-650 nm wavelength range in order to resolve dynamics

from nanosecond to microsecond timescales. Further details about the TA setup can be found in the supporting information.

### Ru complexes

Figure 5a shows the TA surface obtained for monometallic Ru complex **4a**. The surface is described by monoexponential decay of a single excited state species with a monoexponential time constant of 440 ns, as further detailed via the global fitting in the supporting information. The TA spectrum shown in Figure 5c is characterized by three features; a negative  $\Delta A$  feature centered at 450 nm is the expected ground-state bleach associated with the MLCT transition. This feature is flanked by excited state absorption features (positive  $\Delta A$ ) on either side, which are also characteristic of the <sup>3</sup>MLCT excited state in Ru(bpy) derivatives.<sup>28,29</sup> The MLCT excited state appears to involve the bpy ligands rather than the PhIm, which is supported below by the insensitivity of the initial TA spectrum to the substituents on the PhIm ligand in **6** and **7** when the PhIm bridges two metal complexes. The lifetime of this excited state is shortened to 180 ns upon exposure to air, consistent with its triplet spin multiplicity. The absence of additional excited state spectra show that the monometallic complex **4a** has a well-behaved <sup>3</sup>MLCT excited state that decays without forming other photochemical products.

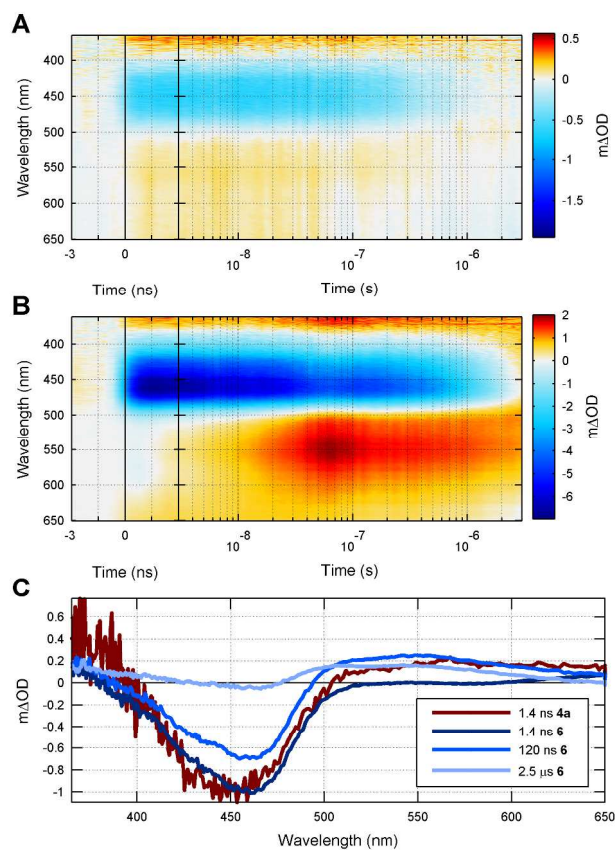


**Figure 5.** a) TA surface for **4a**, and b) TA surface for **6**, both following 355 nm, 700 ps excitation in deaerated conditions. c) Spectral slices from the TA surfaces for **4a** and **6** at the times indicated to compare the nature of the initial and intermediate TA spectra. Globally fitted lifetimes are provided in Table 2.

Figure 5b shows the TA surface for bimetallic Ru-Pt complex **6** under the same conditions as **4a**. The TA spectrum of the

bimetallic complex (Figure 5c) closely resembles that of the monometallic compound for the first few nanoseconds after excitation, pointing to a common excited state – the  $^3\text{MLCT}$  state centered on the  $\text{Ru}(\text{bpy})_2$  component that is common for **4a** and **6**. However, in the case of the dimer, the spectrum undergoes changes with a time constant of 20 ns. This intermediate subsequently decays with a time constant of 1.9  $\mu\text{s}$ , substantially outliving the monometallic complex **4a**. The intermediate in **6** decays to a residual spectrum whose decay cannot be further resolved in this experiment. The new intermediate spectrum (also included in Figure 5c as the 120 ns spectrum) retains a ground-state bleach feature near 450 nm and exhibits a strong new photoinduced absorption feature in the 500–600 nm range. Retention of the ground-state bleach is evidence that the Ru component remains involved in the intermediate state, thus precluding energy transfer to the Pt component. Literature indicates that in monometallic  $\text{phenRu}(\text{bpy})_2$ , an electron from the Ru is transferred to one of the bpy ligands under MLCT excited state and not to the phen.<sup>30</sup> It has been shown that incorporation of ethynyl gold ligands on a phenanthroline can induce charge injection from the Ru into the Au system but only with the ethynyl gold in specific positions on the phen unit.<sup>31</sup> Very similar results are obtained for bimetallic Ru–Pt complex **7** (surfaces contained in the supporting information). Interestingly, we observe that the intermediate state was not formed when **7** was measured under ambient conditions without degassing, rather the initial excited state decayed with approximately the same time constant as **4a** under the same aerated conditions. The globally fitted lifetimes are summarized in table 2.

**Table 2.** Globally fitted TA excited state lifetimes for Ru complexes **4a**, **6**, and **7**.

Complex	$\tau_1$ (ns)	$\tau_2$ ( $\mu\text{s}$ )
<b>4a</b>	440	-
<b>4a*</b>	180	-
<b>6</b>	20	1.9
<b>7</b>	30	2.7
<b>7*</b>	200	-

\*under ambient aerated conditions

### Re complexes

Figure 6a shows the TA surface obtained for monometallic Re complex **4b**. Similar to the Ru complex above, the surface is well described by the monoexponential decay of a single excited state species, whose spectrum is shown in Figure 6c. The spectrum is dominated by two strong photoinduced absorption features; one on the ultraviolet edge of the spectrum around 350 nm, and the other spanning much of the visible region, peaked at around 550 nm. It is likely that the dip between these two peaks near 450 nm contains an overlapping contribution of ground-state bleach from the MLCT transition. The spectrum and its 60 ns lifetime is in line with related  $\text{Re}(\text{phen})(\text{CO})_3\text{Cl}$  complexes.<sup>32</sup> As was the case for the monometallic Ru complex **4a** (above), the monometallic Re species **4b** decays without forming any other photochemical intermediates, and its  $^3\text{MLCT}$  character is confirmed via the accelerated decay under aerated conditions.

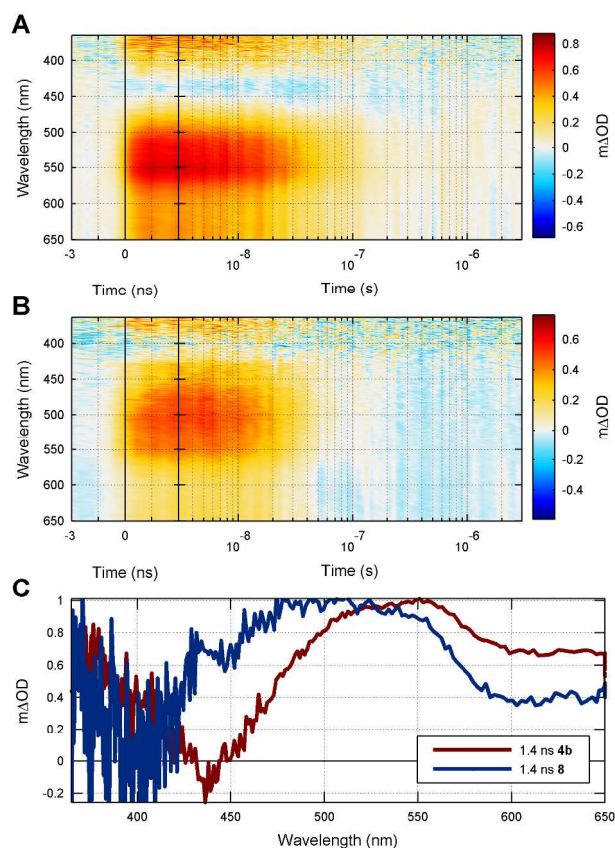


**Figure 6.** a) TA surface for **4b**, and b) TA surface for **8**, both following 355 nm, 700 ps excitation in deaerated conditions. c) Spectral slices from the TA surfaces for **4b** and **8** at the times indicated. Globally fitted lifetimes are provided in Table 3.

**Table 3.** Globally fitted TA excited state lifetimes for Re complexes **4b** and **8**

Complex	$\tau_1$ (ns)
<b>4b</b>	60
<b>4b*</b>	50
<b>8</b>	30
<b>8*</b>	30

\*under ambient aerated conditions

Finally, we examined the bimetallic Re–Pt complex **8**. Unlike the Ru–Pt complexes above that also contain bpy ligands, the primary MLCT excited state for the Re–Pt complex must involve the bridging PhIm ligand. This is reflected by the shift in absorption spectrum induced by the Pt complex on the PhIm ligand, see Figure 2. Consequently, we see that the primary excited state of Re–Pt complex **8** is shifted with respect to the monometallic Re complex **4b**. Nevertheless, the spectrum has broadly the same features; two photoinduced absorption features with an overlapping ground-state bleach in between. These features are all shifted to higher energy for **8** compared with **4b**, in line with the differences in ground-state absorption spectra shown in Figure 2. The excited state decays to the ground-state with a monoexponential time constant of 30 ns – faster than the monometallic complex **4b**, but without producing other intermediates. Thus, we conclude that the excited state spectrum in **8** has the same origin as **4**. The Pt

component in **8** perturbs the excited state energy and lifetime because it is coupled to the PhIm ligand occupied by the MLCT state. However, we find that the Pt component does cause the formation of a new photochemical intermediate.

### Conclusions

In conclusion, we have reported a new synthesis of dimetallic N-heterocyclic carbene/phenanthroline complexes. These new metal complexes have been characterized with absorbances ranging from 395 to 450 nm with fluorescence from 550-675 nm with quantum yields being higher for the ruthenium containing complexes. Time resolved spectroscopy revealed interesting excited state lifetime changes when the NHC metal is varied, however the excited state features are dominated by the metal on the N,N' phenanthroline ligand. Our work has also indicated that the specific metal bound to the phenanthroline moiety is important to the photophysical characteristics of this system. At this point, it is speculative to state whether the bipyridine ligands on the ruthenium are problematic and need replacing. And in view of the importance of this in terms of dual-metal catalysis, we are synthesizing additional complexes and analogs, which will be reported along with their properties and catalytic abilities in the future.

### Experimental

**General:** All reagents were ACS grade and were used without further purification. All reactions were conducted in a dried apparatus under an argon atmosphere unless otherwise stated. Solvents were dried and purified before use, according to standard procedures. Reaction progress was monitored using precoated TLC plates with silica UV254 and visualized by UV radiation ( $\lambda = 254$  nm). Flash column chromatography was performed using silica gel C60 (220-240 mesh) with the solvent systems as indicated.

$^1\text{H}$  and  $^{13}\text{C}$  NMR spectra were recorded with deuterated solvents using a Bruker 400 or 600 MHz NMR spectrometer, calibrated using the stated residual protonated solvent as an internal reference. Chemical shifts ( $\delta$ ) are reported in parts per million (ppm) and coupling constants ( $J$ ) are measures in hertz (Hz). Fourier-transform infrared (FT-IR) spectroscopy was performed with a Perkin Elmer Spectrum One spectrometer using freshly prepared potassium bromide. See supporting information for detailed instrument and procedures for physical measurements including Fluorescence spectroscopy, Time-Correlated Single Photon Counting measurements and Transient Absorption Spectroscopy.

**Pentyl-imidazo[4,5-f][1,10]phenanthroline – 2.** A 25 ml flask was loaded with 1*H*-imidazo[4,5-*f*][1,10]phenanthroline **1** (800 mg, 3.635 mmol), sodium hydroxide (157 mg, 3.926 mmol), and DMSO (16 ml). The solution was stirred for 2 h at rt after which 1-iodopentane was added (500  $\mu\text{l}$ , 3.816 mmol) and the solution continued to stir for an additional 25 m. The solution was heated to 37 °C and stirred overnight. The solution was cooled to rt and dissolved in water (25 ml), washed with methylene chloride (3 x 15 ml), dried with  $\text{MgSO}_4$ , and filtered. The resulting solution was concentrated to a solid. Pure product was obtained through recrystallization with  $\text{CH}_2\text{Cl}_2/\text{Et}_2\text{O}$  at 0 °C to yield **2** as a brown solid (856 mg, 80%)  $^1\text{H}$  NMR:  $\text{CDCl}_3$ :  $\delta$  9.16 (d,  $J =$  Hz, 2H), 9.00 (dd,  $J = 8.09, 1.8$  Hz, 1H), 8.57 (dd,  $J = 8.36, 1.56$  Hz, 1H), 8.02 (s, 1H), 7.77 (dd,  $J = 8.08, 4.36$  Hz, 1H), 7.63 (dd,  $J = 8.37, 4.37$  Hz, 1H), 4.64 (t,  $J = 7.20$  Hz, 2H), 2.08 (pentet, 2H), 1.47 (sextet, 4H), 0.95 (t,  $J = 14.09$  Hz, 3H) ppm.  $^{13}\text{C}$  NMR  $\text{CDCl}_3$ :  $\delta$  148.6, 147.7, 144.5, 143.9, 142.6, 137.3, 130.0, 128.0, 124.2, 123.5, 123.3, 122.4, 119.6, 47.8 (NCH<sub>2</sub>), 29.5 (NCH<sub>2</sub>CH<sub>2</sub>), 28.5 (NCH<sub>2</sub>CH<sub>2</sub>CH<sub>2</sub>), 22.0 (CH<sub>2</sub>CH<sub>3</sub>), 13.7 (CH<sub>3</sub>) ppm. Anal. Calcd. for  $\text{C}_{18}\text{H}_{18}\text{N}_4$ : C, 74.46; H,

6.25; N, 19.30. Found: C, 74.66; H, 6.15; N, 19.21.

**1-pentyl-imidazo[4,5-f][1,10]phenanthroline ruthenium (bpy)<sub>2</sub> dichloride - 3a.** A 50 ml flask was loaded with 1-pentyl-1*H*-imidazo[4,5-*f*][1,10]phenanthroline (570 mg, 1.923 mmol), cis-(bpy)<sub>2</sub>RuCl<sub>2</sub>·2H<sub>2</sub>O (1.00 mg, 1.932 mmol), and EtOH/H<sub>2</sub>O (35 ml) 4:1. The stirred solution was heated at reflux for 7 h then cooled to rt and concentrated to a solid. Recrystallization from ethanol at 0 °C yielded **3a** as a red solid (1.164 mg, 78%).  $^1\text{H}$  NMR: DMSO-*d*<sup>6</sup>:  $\delta$  9.06 (dd,  $J = 8.40, 1.20$  Hz, 1H), 8.99 (d,  $J = 8.48$  Hz, 1H), 8.87 (dd,  $J = 15.96, 8.2$  Hz, 4H), 8.70 (s, 1H), 8.23 (t,  $J = 7.81$  Hz, 2H), 8.10 (m, 4H), 7.92 (m, 4H), 7.83 (t,  $J = 4.92$  Hz, 2H), 7.60 (m, 4H), 7.33 (m, 2H), 4.81 (t,  $J = 7.04$  Hz, 2H), 1.94 (pentet, 2H), 1.35 (comp, 4H), 0.87 (t,  $J = 6.96$  Hz, 3H) ppm.  $^{13}\text{C}$  NMR: DMSO-*d*<sup>6</sup>:  $\delta$  156.8, 156.7, 156.6, 151.4, 151.4, 151.3, 150.2, 149.6, 146.3, 145.2, 145.1, 138.0, 137.9, 137.4, 130.3, 130.2, 128.0, 127.9, 127.8, 127.7, 126.7, 126.3, 125.9, 124.7, 124.7, 124.6, 121.6, 47.1, 29.3, 28.0, 21.6, 13.8 ppm. Anal. Calcd. for  $\text{C}_{38}\text{H}_{34}\text{Cl}_2\text{N}_8\text{Ru}$ : C, 58.91; H, 4.42; N, 14.46. Found: C, 59.28; H, 4.38; N, 14.89.

### 3-methyl-1-pentyl-phenanthro[1,10-f][4,5]imidazolium

**ruthenium (bpy)<sub>2</sub> dichloride iodide.** A schlenk tube was loaded with 1-pentyl-imidazo[4,5-*f*][1,10]phenanthroline ruthenium (bpy)<sub>2</sub> dichloride (250 mg, 0.332 mmol) and dimethylformamide (6 ml). Iodomethane (200  $\mu\text{l}$ , 3.221 mmol) was then added, the flask was sealed and heated to 100 °C with stirring for 2 d. The solution was cooled to rt, solvent was evaporated under high vacuum and the solid was recrystallized from ethanol at 0 °C to give a red solid (213 mg, 72%).  $^1\text{H}$  NMR: DMSO-*d*<sup>6</sup>:  $\delta$  10.05 (s, 1H), 9.33 (d,  $J = 8.48$  Hz, 1H), 9.19 (d,  $J = 8.21$  Hz, 1H), 8.93 (m, 4H), 8.31 (d,  $J = 4.76$  Hz, 2H), 8.23 (t,  $J = 7.84$  Hz, 2H), 8.12 (t,  $J = 8.28$  Hz, 2H), 8.06 (m, 2H), 7.82 (m, 2H), 7.60 (m, 4H), 7.36 (t,  $J = 6.20$  Hz, 2H), 4.99 (t,  $J = 6.96$  Hz, 2H), 4.60 (s, 3H), 2.08 (m, 2H), 1.50 (m, 2H), 1.42 (m, 2H), 0.93 (t,  $J =$  Hz, 3H) ppm.  $^{13}\text{C}$  NMR DMSO-*d*<sup>6</sup>:  $\delta$  162.7, 157.0, 157.0, 153.1, 153.0, 152.1, 152.0, 152.0, 151.9, 146.8, 146.8, 144.6, 138.7, 138.6, 131.9, 128.5, 128.5, 128.3, 128.3, 127.9, 127.6, 127.1, 125.8, 125.1, 125.0, 121.4, 121.1, 50.5, 38.5, 34.8, 28.1, 22.1, 14.2 ppm. DEPT90 DMSO-*d*<sup>6</sup>:  $\delta$  153.1, 153.0, 152.0, 151.9, 151.8, 138.7, 138.5, 131.9, 128.4, 128.2, 127.9, 127.5, 125.1, 125.0 ppm. Anal. Calcd. for  $\text{C}_{39}\text{H}_{37}\text{Cl}_2\text{IN}_8\text{Ru}$ : C, 51.10; H, 4.07; N, 12.22. Found: C, 51.29; H, 4.31; N, 12.59.

### 3-methyl-1-pentyl-phenanthro[1,10-f][4,5]imidazolium

**ruthenium (II) bis-2,2'-bipyridine tris tetraphenyl borate - 4a.** Under an air atmosphere, 3-methyl-1-pentyl-phenanthro[1,10-*f*][4,5]imidazolium ruthenium (bpy)<sub>2</sub> dichloride iodide (600 mg, 0.653 mmol) and sodium tetraphenyl borate (670 mg, 1.958 mmol) were dissolved in acetonitrile (50 ml). The solution was stirred for 10 min and concentrated to a solid. The solid was washed with ethanol and isolated through vacuum filtration to yield **4a** as an orange solid (560 mg, 51%).  $^1\text{H}$  NMR: DMSO-*d*<sup>6</sup>:  $\delta$  10.05 (s, 1H), 9.24 (d,  $J = 7.76$  Hz, 1H), 9.15 (d,  $J = 7.88$  Hz, 1H), 8.86 (comp, 4H), 8.26 (comp, 4H), 8.07 (t,  $J = 14.00, 6.40$  Hz, 2H), 7.80 (t,  $J = 8.80, 5.20$  Hz, 2H), 7.96 (comp, 2H), 7.53 (comp, 4H), 7.30 (comp, 2H), 7.19 (s, 24H), 6.93 (t,  $J = 14.80, 7.20$  Hz, 24H), 6.80 (t,  $J = 14.40, 7.20$  Hz, 12H), 4.94 (t, 2H), 4.54 (s, 3H), 2.05 (pentet, 2H), 1.49 (pentet, 2H), 1.40 (sextet, 2H), 0.94 (t, 3H) ppm.  $^{13}\text{C}$  NMR: Acetone-*d*<sup>6</sup>: 164.5, 164.4, 164.3, 164.2, 164.1, 164.0, 163.9, 163.8, 163.7, 163.6, 161.9, 156.9, 156.9, 153.0, 152.9, 151.7, 147.0, 138.4, 138.2, 136.1, 136.1, 131.2, 128.7, 127.9, 127.8, 127.4, 127.2, 127.0, 126.1, 126.2, 125.1, 124.6, 124.6, 121.3, 50.8, 39.1, 35.2, 28.53, 21.9, 12.9 ppm. IR (KBr): 3056, 3000  $\text{cm}^{-1}$ . Anal. Calcd. for  $\text{C}_{111}\text{H}_{97}\text{B}_3\text{N}_8\text{Ru}$ : C, 79.52; H, 5.83; N, 6.68. Found: C, 79.28; H, 5.40; N, 6.39.

**Silver bis-3-methyl-1-pentyl-phenanthro[1,10-f][4,5]imidazolium ruthenium (II) bis-2,2'-bipyridine bis tetraphenyl borate - 5a.** A 50 ml flask was loaded with 3-methyl-1-pentyl-phenanthro[1,10-f][4,5]imidazolium ruthenium (II) bis-2,2'-bipyridine tris tetraphenyl borate (2.089 g, 1.245 mmol), silver oxide (289 mg, 1.246 mmol), and methylene chloride (25 ml). The solution was stirred at rt in darkness for 17 h. The resulting precipitate was filtered and washed with methylene chloride to yield **5a** as an orange solid (1.938 g, 87%). <sup>1</sup>H NMR DMSO-d<sub>6</sub>: δ 9.33 (d, *J* = 8.96 Hz, 2H), 9.09 (d, *J* = 8.8 Hz, 2H), 8.88 (comp, 8H), 8.24 (comp, 8H), 8.12 (t, *J* = 16.09, 7.97 Hz, 4H), 8.00 (comp, 2H), 7.83 (t, *J* = 11.25, 5.56 Hz, 4H), 7.59 (comp, 9H), 7.33 (t, *J* = 13.16, 7.08 Hz, 5H), 7.18 (s, 48H), 6.93 (t, *J* = 14.68, 7.32 Hz, 48H), 6.80 (t, *J* = 14.28, 7.16 Hz, 24H), 5.07 (t, 2H), 4.65 (s, 3H), 1.99 (pentet, 2H), 1.54 (pentet, 2H), 1.39 (sextet, 2H), 0.90 (t, 3H) ppm.

**1-pentyl-imidazo[4,5-f][1,10]phenanthroline rhenium tricarbonyl chloride - 3b.** A 25 ml flask was loaded with 1-pentyl-imidazo[4,5-f][1,10]phenanthroline **2** (200 mg, 0.675 mmol), rhenium pentacarbonyl chloride (232 mg, 0.643 mmol), and toluene (8 ml). The solution was heated to 80 °C and stirred overnight. The solution was cooled to rt and the precipitate was isolated via vacuum filtration and washed with diethyl ether. The yellow solid was dissolved in methylene chloride and concentrated to a solid. Purification was achieved through recrystallization with CH<sub>2</sub>Cl<sub>2</sub>/Et<sub>2</sub>O at 0 °C overnight to yield **3b** as a yellow solid (356 mg, 93%). <sup>1</sup>H NMR CDCl<sub>3</sub>: δ 9.42 (dd, *J* = 5.08, 1.24 Hz, 1H), 9.39 (dd, *J* = 5.12, 1.48 Hz, 1H), 9.25 (dd, *J* = 8.28, 1.48 Hz, 1H), 8.80 (dd, *J* = 8.52, 1.20 Hz, 1H), 8.18 (s, 1H), 7.973 (ddd, *J* = 16.49, 9.17, 5.09 Hz, 2H), 4.68 (t, *J* = 5.8 Hz, 2H), 2.08 (m, 2H), 1.47 (m, 4H), 0.97 (t, *J* = 6.89 Hz, 3H) ppm. <sup>13</sup>C NMR DMSO-d<sub>6</sub>: δ 198.3, 198.2, 190.4, 152.2, 151.5, 146.8, 144.4, 144.2, 137.3, 133.2, 133.1, 127.4, 126.8, 126.2, 124.5, 122.0, 47.4, 29.5, 28.4, 22.12, 14.32 ppm. Anal. Calcd. for C<sub>21</sub>H<sub>18</sub>ClN<sub>4</sub>O<sub>3</sub>Re: C, 42.32; H, 3.04; N, 9.40. Found: C, 42.68; H, 2.99; N, 9.48.

**3-methyl-1-pentyl-phenanthro[9,10-f][4,5]imidazolium iodide rhenium tricarbonyl chloride.** A schlenk tube was loaded with 1-pentyl-imidazo[4,5-f][1,10]phenanthroline rhenium tricarbonyl chloride (550 mg, 0.923 mmol) and dimethylformamide (12 ml). Iodomethane (287 μl, 4.613 mmol) was then added and the flask was sealed and heated to 100 °C stirring for 3 d. The solvent was evaporated under high vacuum and the solid was isolated via vacuum filtration, washing with methylene chloride (50 ml), to yield an orange solid (586 mg, 86%) after drying. <sup>1</sup>H NMR: DMSO-d<sub>6</sub>: δ 10.06 (s, 1H), 9.67 (d, *J* = 5.2 Hz, 2H), 9.52 (d, *J* = 8.16 Hz, 1H), 9.39 (d, *J* = 8.96 Hz, 2H), 8.30 (m, 2H), 5.04 (t, *J* = 7.77 Hz, 2H), 4.63 (s, 3H), 2.06 (m, 2H), 1.49 (m, 2H), 1.41 (m, 2H), 0.93 (t, *J* = 7.16 Hz, 3H) ppm. <sup>13</sup>C NMR DMSO-d<sub>6</sub>: δ 196.9 (CO), 196.8 (CO), 188.9 (CO), 154.8 (ArCH), 154.7 (ArCH), 145.6, 145.5, 144.5 (ArCH), 134.7 (ArCH), 134.6 (ArCH), 127.9 (ArCH), 127.6 (ArCH), 126.7, 125.2, 121.4, 121.1, 50.6 (NCH<sub>2</sub>), 38.5 (NCH<sub>3</sub>), 28.4 (NCH<sub>2</sub>CH<sub>2</sub>), 28.2 (NCH<sub>2</sub>CH<sub>2</sub>CH<sub>2</sub>CH<sub>2</sub>), 22.2 (CH<sub>2</sub>CH<sub>2</sub>CH<sub>3</sub>), 14.3 (CH<sub>2</sub>CH<sub>3</sub>). IR (KBr): 2027, 1930, 1907 cm<sup>-1</sup>. Anal. Calcd. for C<sub>22</sub>H<sub>21</sub>ClIN<sub>4</sub>O<sub>3</sub>Re: C, 35.81; H, 2.87; N, 7.59. Found: C, 35.55; H, 3.01; N, 7.40.

**3-methyl-1-pentyl-phenanthro[9,10-f][4,5]imidazolium tetraphenyl borate rhenium tricarbonyl chloride - 4b.** Under an air atmosphere, 3-methyl-1-pentyl-phenanthro[9,10-f][4,5]imidazolium iodide rhenium tricarbonyl chloride (500 mg, 0.676 mmol) was dissolved in acetonitrile (50 ml) and sodium tetraphenyl borate (231 mg, 0.676 mmol) was added. The solution

was stirred for 15 min, filtered through diatomaceous earth to remove the halide salts, and concentrated. Recrystallization with CH<sub>2</sub>Cl<sub>2</sub>/Et<sub>2</sub>O at 0 °C followed by vacuum filtration gave **4b** as an orange solid (362 mg, 58%). <sup>1</sup>H NMR DMSO-d<sub>6</sub>: δ 10.05 (s, 1H), 9.67 (d, *J* = 5.12 Hz, 2H), 9.51 (d, *J* = 8.05 Hz, 1H), 9.39 (d, *J* = 8.28 Hz, 1H), 8.31 (ddd, *J* = 11.56, 8.6, 6.12 Hz, 2H), 7.18 (d, *J* = 1.32 Hz, 8H), 6.94 (t, *J* = 7.32 Hz, 8H), 6.80 (t, *J* = 7.21 Hz, 4H), 5.04 (m, 2H), 4.63 (s, 3H), 2.07 (m, 2H), 1.47 (comp, 4H), 0.94 (t, *J* = 7.2 Hz, 3H) ppm. <sup>13</sup>C NMR: DMSO-d<sub>6</sub>: δ 196.4, 188.4, 164.1, 163.6, 163.1, 162.6, 154.3, 154.2, 145.1, 145.1, 144.2, 135.5, 134.1, 133.9, 128.9, 127.4, 127.1, 126.7, 126.3, 125.3, 125.3, 124.9, 121.6, 120.9, 120.6, 50.2, 38.1, 27.9, 27.7, 21.7, 13.8 ppm. IR (KBr): 2022, 1904 cm<sup>-1</sup>. Anal. Calcd. for C<sub>46</sub>H<sub>41</sub>BClN<sub>4</sub>O<sub>3</sub>Re: C, 59.39; H, 4.44; N, 6.02. Found: C, 58.89; H, 4.28; N, 6.19.

**Silver bis-3-methyl-1-pentyl-phenanthro[9,10-f][4,5]imidazolium tetraphenyl borate rhenium tricarbonyl chloride - 5b.** A 25 ml flask was loaded with 3-methyl-1-pentyl-phenanthro[9,10-f][4,5]imidazolium tetraphenyl borate rhenium tricarbonyl chloride (100 mg, 0.107 mmol) and methylene chloride (5 ml). The stirred solution was cooled to 0 °C, silver oxide (19 mg, 0.081 mmol) was added and the solution stirred in darkness at 0 °C for 2h. After warming to rt and stirring for 17h, a precipitate was isolated through addition of diethyl ether. Vacuum filtration and washing with diethyl ether gave **5b** as a yellow solid (83 mg, 40%). <sup>1</sup>H NMR DMSO-d<sub>6</sub>: δ 9.56 (comp, 6H), 9.34 (d, *J* = 8.8 Hz, 2H), 8.30 (m, 4H), 7.18 (s, 6H), 6.94 (t, *J* = 14.72, 7.28 Hz, 8H), 6.80 (t, *J* = 14.64, 7.08 Hz, 4H), 5.14 (triplet, 2H), 4.17 (s, 3H), 2.00 (quartet, 2H), 1.52 (quartet, 2H), 1.41 (sextet, 2H), 0.90 (t, *J* = 14.17, 7.08 Hz, 3H) ppm.

**Dichloro platinum 3-methyl-1-pentyl-phenanthro[1,10-f][4,5]imidazolium ruthenium (II) bis-2,2'-bipyridine bis tetraphenyl borate - 6.** A 25 ml flask was loaded with silver bis-3-methyl-1-pentyl-phenanthro[1,10-f][4,5]imidazolium ruthenium (II) bis-2,2'-bipyridine bis tetraphenyl borate (75 mg, 0.021 mmol), potassium tetrachloroplatinate (17 mg, 0.042 mmol), dimethyl sulfoxide (4 ml) and stirred overnight at 60 °C. Diethyl ether was added to the solution, the solid was filtered, and washed with diethyl ether to yield **6** as an orange solid (23mg, 29%). <sup>1</sup>H NMR DMSO-d<sub>6</sub>: δ 9.16 (d, *J* = 8.56 Hz, 1H), 8.88 (d, *J* = 8.81 Hz, 1H), 8.53 (m, 4H), 8.47 (m, 2H), 8.10 (t, *J* = 15.37, 7.65 Hz, 2H), 7.99 (t, *J* = 15.76, 7.76 Hz, 2H), 7.84 (m, 4H), 7.55 (m, 2H), 7.44 (m, 2H), 7.28 (16H), 7.22 (m, 4H), 7.01 (t, *J* = 14.6, 7.28 Hz, 16H), 6.98 (t, *J* = 14.2, 7.16 Hz, 8H), 5.94 (m, 1H), 5.33 (m, 1H), 4.91 (s, 3H), 3.58 (dd, *J* = 9.61, 6.61 Hz, 6H), 1.79 (sextet, 2H), 1.55 (pentet, 2H), 1.03 (quartet, *J* = 14.52, 7.2 Hz, 3H) ppm. <sup>13</sup>C CD<sub>3</sub>CN: δ 164.3, 163.9, 163.6, 163.3, 157.0, 156.8, 152.06, 152.02, 151.85, 151.80, 151.77, 151.73, 151.6, 146.0, 138.0, 137.9, 135.7, 131.0, 130.9, 130.7, 127.6, 127.46, 127.43, 127.41, 126.57, 126.53, 126.24, 126.21, 125.62, 125.60, 125.5, 124.4, 124.3, 124.2, 121.7, 121.0, 120.7, 55.2, 43.0, 39.6, 28.5, 28.2, 22.1, 13.3 ppm. IR (KBr): 3048, 1461, 1442, 1398, 732, 705 cm<sup>-1</sup>. Anal. Calcd. for C<sub>89</sub>H<sub>82</sub>B<sub>2</sub>Cl<sub>2</sub>N<sub>8</sub>OPtRuS: C, 62.87; H, 4.86; N, 6.59. Found: C, 63.13; H, 4.39; N, 6.33.

**Platinum (I) 2,2'2''-terpyridine 3-methyl-1-pentyl-phenanthro[1,10-f][4,5]imidazolium ruthenium (II) bis-2,2'-bipyridine bis tetraphenyl borate triflate - 7.** A 25 ml flask was loaded with silver bis-3-methyl-1-pentyl-phenanthro[1,10-f][4,5]imidazolium ruthenium (II) bis-2,2'-bipyridine bis tetraphenyl borate (362 mg, 0.101 mmol) and acetonitrile (9 ml). 2,2'2''-terpyridine platinum (I) chloride triflate (108 mg, 0.203) dissolved in acetonitrile (3 ml) was added dropwise to the reaction mixture and the solution was allowed to stir at rt for 1.5 h. Diethyl ether was added to the reaction mixture and the resulting precipitate was

isolated through vacuum filtration, washing with additional diethyl ether, to yield **7** as an orange solid (193 mg, 70%). <sup>1</sup>H NMR DMSO-d<sub>6</sub>: δ 9.32 (d, *J* = 4.80 Hz, 1H), 9.09 (d, *J* = 8.40 Hz, 1H), 8.88 (comp, 4H), 8.62 (comp, 6H), 8.51 (t, *J* = 14.40, 7.6 Hz, 2H), 8.22 (comp, 4H), 8.12 (t, *J* = 15.20, 7.60 Hz, 2H), 8.00 (comp 4H), 7.83 (t, *J* = 13.20, 6.00 Hz, 2H), 7.57 (comp, 6H), 7.31 (t, *J* = 12.80, 6.80 Hz, 2H), 7.17 (s, 16H), 6.92 (t, *J* = 14.00, 7.20 Hz, 16H), 6.79 (t, *J* = 14.00, 7.20 Hz, 8H), 5.06 (t, 2H), 4.64 (s, 3H), 2.07 (pentet, 2H), 1.54 (pentet, 2H), 1.39 (sextet, 3H), 0.90 (t, *J* = 14.00, 6.80 Hz, 3H) ppm. <sup>13</sup>C NMR DMSO-d<sub>6</sub>: δ 164.3, 164.0, 163.7, 163.6, 163.3, 159.2, 159.1, 158.7, 157.0, 154.8, 154.7, 154.3, 151.7, 151.5, 146.0, 145.6, 145.7, 143.5, 143.1, 142.5, 138.7, 138.6, 138.4, 135.9, 131.9, 131.7, 131.3, 130.2, 129.7, 129.6, 128.7, 128.4, 128.2, 128.1, 127.7, 127.5, 127.2, 127.0, 126.9, 126.7, 126.3, 125.8, 125.7, 125.1, 125.0, 124.9, 122.0, 121.9, 121.4, 121.3, 120.9, 120.8, 120.0, 54.9, 41.3, 40.6, 29.4, 28.6, 23.30, 23.4, 14.3 ppm. IR (KBr): 3058, 3000, 1481, 737, 710 cm<sup>-1</sup>. Anal. Calcd. for C<sub>103</sub>H<sub>87</sub>B<sub>2</sub>F<sub>3</sub>N<sub>11</sub>O<sub>3</sub>PtRu: C, 65.06; H, 4.61; N, 8.10. Found: C, 65.54; H, 4.20; N, 8.35.

**Dichloro platinum 3-methyl-1-pentyl-phenanthro[1,10-f][4,5]imidazolium rhenium tricarbonyl chloride tetraphenyl borate – 8.** A 25 ml flask was loaded with silver bis-3-methyl-1-pentyl-phenanthro[9,10-f][4,5]imidazolium tetraphenyl borate rhenium tricarbonyl chloride (75 mg, 0.038 mmol) and potassium tetrachloroplatinate (II) (32 mg, 0.076 mmol) and dimethyl sulfoxide (3ml). The solution was heated to 60 °C, stirred in darkness for 17 h then cooled to rt. DMSO was removed under vacuum and the remaining solid was dissolved in methylene chloride and precipitated via slow addition of diethyl ether followed by vacuum filtration to yield **8** as a yellow solid (67 mg, 69%). <sup>1</sup>H NMR CD<sub>3</sub>CN: δ 9.48 (dd, *J* = 2.80, 1.20 Hz, 2H), 9.36 (dd, *J* = 8.40, 2.40 Hz, 1H), 9.08 (d, *J* = 8.40 Hz, 1H), 8.15 (m, 1H), 8.07 (m, 1H), 7.30 (s, 4H), 7.03 (t, *J* = Hz, 4H), 6.87 (t, *J* = Hz, 2H), 5.52 (m, 1H), 5.32 (m, 1H), 4.90 (s, 3H), 2.04 (m, 1H), 1.73 (pentet, 2H), 1.53 (sextet, 2H), 1.02 (t, *J* = Hz, 3H) ppm. <sup>13</sup>C NMR CD<sub>3</sub>CN: δ 198.2, 189.5, 164.3, 163.9, 163.6, 163.3, 152.6, 152.5, 145.0, 135.7, 133.6, 133.6, 133.2, 133.1, 128.3, 127.2, 126.7, 126.3, 121.7, 120.6, 120.6, 51.3, 45.6, 45.6, 45.1, 39.6, 28.5, 28.2, 22.1, 13.3 ppm. IR (KBr): 2024, 1919 cm<sup>-1</sup>. Anal. Calcd. for C<sub>48</sub>H<sub>46</sub>BCl<sub>3</sub>N<sub>4</sub>O<sub>4</sub>PtReS: C, 45.27; H, 3.64; N, 4.40. Found: C, 45.01; H, 3.88; N, 4.19.

## Acknowledgements

This work was supported by the University of Wyoming, School of Energy Resources, the Center for Photoconversion and Catalysis and an NSF EAPSI fellowship for A. Pearson, Grant No. 1316751.

## Notes and references

<sup>a</sup> Department of Chemistry, University of Wyoming, Laramie, WY 82071

<sup>b</sup> MacDiarmid Institute of Advanced Materials and Nanotechnology, School of Chemical and Physical Sciences, Victoria University of Wellington, New Zealand.

Electronic Supplementary Information (ESI) available: Fluorescence and Transient absorption spectroscopy and NMR spectra. See DOI: 10.1039/b000000x/

1. A. Duschek and S. F. Kirsch, *Angew. Chem. Int. Ed.*, 2008, **47**, 5703-5705.
2. J. J. Hirner, Y. Shi and S. A. Blum, *Acc. Chem. Res.*, 2011, **44**, 603-613.

3. J. Ji, X. Zhang, Y. Zhu, Y. Qian, J. Zhou, L. Yang and W. Hu, *J. Org. Chem.*, 2011, **76**, 5821-5824.
4. G. M. Sammis, H. Danjo and E. N. Jacobsen, *J. Am. Chem. Soc.*, 2004, **126**, 9928-9929.
5. E. K. van den Beuken and B. L. Feringa, *Tetrahedron*, 1998, **54**, 12985-13011.
6. D. Astruc, *Acc. Chem. Res.*, 1997, **30**, 383-391.
7. G. De Ruiter and M. E. Van Der Boom, *Acc. Chem. Res.*, 2011, **44**, 563-573.
8. Z. Ji, S. Li, Y. Li and W. Sun, *Inorg. Chem.*, 2010, **49**, 1337-1346.
9. N. J. Long, *Angew. Chem. Int. Ed. Eng.*, 1995, **34**, 21-38.
10. I. R. Whittall, A. M. Donagh, M. G. Humphrey and M. Samoc, *Adv. Organomet. Chem.*, 1998, **42**, 291-362.
11. S. Chakraborty, T. J. Wadas, H. Hester, R. Schmehl and R. Eisenberg, *Inorg. Chem.*, 2005, **44**, 6865-6878.
12. P. Du and R. Eisenberg, *Energy Environ. Sci.*, 2012, **5**, 6012-6021.
13. S. Diez-Gonzalez, N. Marion and S. P. Nolan, *Chem. Rev.*, 2009, **109**, 3612-3676.
14. M. Poyatos, J. A. Mata and E. Peris, *Chem. Rev.*, 2009, **109**, 3677-3707.
15. W. A. Herrmann, M. Ellison, J. Fischer, C. Kocher and G. R. J. Artus, *Angew. Chem. Int. Ed. Eng.*, 1995, **34**, 2371-2374.
16. M. Mechler, K. Latendorf, W. Frey and R. Peters, *Organometallics*, 2013, **32**, 112-130.
17. S. Shrestha, C. Gimbert-Surinach, M. Bhadbhade and S. B. Colbran, *Eur. J. Inorg. Chem.*, 2011, 4331-4337.
18. H.-J. Park and Y. K. Chung, *Inorg. Chem. Acta*, 2012, **391**, 105-113.
19. H.-J. Park, W. Kim, W. Choi and Y. K. Chung, *New J. Chem.*, 2013, **37**, 3174-3182.
20. C.-Y. Chen, H.-C. Lu, C.-G. Wu, J.-G. Chen and K.-C. Ho, *Adv. Funct. Mat.*, 2007, **17**, 29-36.
21. W. Paw and R. Eisenberg, *Inorg. Chem.*, 1997, **36**, 2287-2293.
22. J.-Z. Wu, B.-H. Ye, L. Wang, L.-N. Ji, J.-Y. Zhou, R.-H. Li and Z.-Y. Zhou, *J. Chem. Soc. Dalton Trans.*, 1997, 1395-1401.
23. B. P. Sullivan, D. J. Salmon and T. J. Meyer, *Inorg. Chem.*, 1978, **17**, 3334-3341.
24. H. M. J. Wang and I. J. B. Lin, *Organometallics*, 1998, **17**, 972-975.
25. C. P. Newman, R. J. Deeth, G. J. Clarkson and J. P. Rourke, *Organometallics*, 2007, **26**, 6225-6233.
26. G. Ajayakumar, M. Kobayashi, S. Masaokaa and K. Sakai, *Dalton Trans.*, 2011, **40**, 3955-3966.
27. Demas, J. N. and Crosby, G. A. *J. Am. Chem. Soc.* 1971, **93**, 2841-2847.
28. Kober, E. M. and Meyer, T. J. *Inorg. Chem.* 1982, **21**, 3967-3977.
29. McCusker, J. K. *Acc. Chem. Res.* 2003, **36**, 876-887
30. Chang, Y. J.; Xu, X.; Yabe, T.; Yu, S. C.; Anderson, D. R.; Orman, L. K. and Hopkins, J. B. *J. Phys. Chem.* 1990, **94**, 729-736

31. Shiotsuka, M.; Tsuji, Y.; Keyaki, K. and Nozaki, K. *Inorg. Chem.* 2010, **49**, 4186-4193.
32. Sato, S.; Morimoto, T. and Ishitani, O. *Inorg. Chem.* 2007, **46**, 9051-9053.

